

Diffusion Tensor Imaging with Highly constrained backProjection (HYPR)

A. L. Alexander¹, J. Lee¹, C. A. Mistretta¹

¹Medical Physics, University of Wisconsin, Madison, WI, United States

Diffusion Tensor Imaging with Highly constrained backProjection (HYPR)

Introduction:

Diffusion tensor imaging (DTI) and other DW imaging methods are typically applied using echo-planar imaging (EPI) methods, which are highly efficient and insensitive to motion, but are prone to significant artifacts including image distortion, blurring and ghosting. Conversely, diffusion-weighted projection reconstruction imaging (DW-PRI) methods [1-4] demonstrate significantly reduced image artifacts; however, the scans are significantly slower and much less noise efficient. The imaging time requirements of DW-PRI are particularly prohibitive for DW scans using a large number diffusion encoding directions, such as q-ball imaging (QBI) and diffusion spectrum imaging (DSI) [5]. In this study, a novel image reconstruction method, HYPR (highly constrained backprojection) [6], was used to reconstruct diffusion tensor images from a set of highly undersampled DW PRI data. HYPR is a method in which a series of angularly undersampled images are obtained in projection mode. For each image in the series a highly constrained back projection technique is used in which the backprojected signal is deposited only in those locations provided by a composite image that is formed from the set of all interleaved sets of projections acquired in the entire scan [6].

Methods:

The acquisition of the undersampled DW-PRI data was simulated using real DTI data acquired using a DW-EPI pulse sequence with 100 encoding directions generated by an analytic approach that smoothly sweeps the surface of a sphere in a uniform pattern [7]. This trajectory was used to change the DW signal intensities slowly, which is important for the HYPR reconstruction. The images were acquired at 3.0 Tesla using an 8-channel head receiver coil, single-shot DW EPI pulse sequence with bipolar gradients and dual-echo refocusing, SENSE parallel imaging with a reduction factor of two, cardiac gating with the effective TR equal to 3 heartbeats (~3 s), a single 4 mm thick slice, 240 mm FOV, and 128x128 acquisition interpolated to 256x256. Two sets of image data were collected with b-values of 1000 and 8000 s/mm² in addition to a reference image with b = 0 s/mm². Maps of mean diffusivity, FA, and the major eigenvector were computed. This data was then used to simulate the acquisition of DW-PRI data. For each directionally-encoded input image, a series of 20 projections were generated by Radon transformation. Prior to this, the input image noise variance was increased by a factor of twenty to simulate the lower SNR that would be obtained with 20 rather than the 400 projections required by the Nyquist theorem. The undersampling achieved with HYPR is most effective when the image regions of changing signal are sparse. To increase the sparsity of the image sequence, each image was subtracted from the average of its two nearest neighbors in the sequence. Following HYPR processing, this information was added back to generate the final estimate of each directional image. The DW HYPR images were then combined to estimate the diffusion tensor at each voxel location and maps of the mean diffusivity, FA and major eigenvector direction were estimated.

Results:

The effects of the HYPR reconstruction on DTI data are shown in Figure 1 for one DW image in the b=1000s/mm² data set. Images that were reconstructed using standard filtered backprojection from the 20 projections clearly demonstrate significant streaking and aliasing artifacts. Even though additional noise was added to the input data, the HYPR reconstruction improved the image SNR of the individual frames. Overall, the acquisition speed was increased by a factor of 20 using the HYPR reconstruction. The FA, mean diffusivity and major eigenvector maps from the original and HYPR data are shown in Figure 2. The errors in the mean diffusivity is relatively small (see plot in Figure 3). However, the estimates of FA from HYPR appear to be somewhat noisier as indicated by the dispersion in the FA comparison plot in Figure 3. Although not shown, the results for b=8000s/mm² were similar.

Discussion:

When conventional filtered back projection (FBP) is used to reconstruct the individual undersampled projection sets, the images displayed severe streak artifacts and the SNR from 20 projections is significantly reduced. With HYPR the SNR of the processed images is usually determined by the entire scan time and streaks are significantly reduced. Overall, the mean diffusivity appears to be preserved although the FA values are moderately increased indicating a slight distortion in the reconstructed diffusion tensors. Despite this error, the method is promising for estimates of mean diffusivity and the eigenvector directions for white matter tractography. The distortion in the FA values may be caused by averaging of image intensities across neighboring encodings. If the directional information can be preserved, the method may be promising for new diffusion image processing methods including HARDI with spherical harmonics or q-ball imaging.

Conclusions:

We have demonstrated that HYPR is promising for dramatically improving the acquisition speed of DW-PRI data. In this study, an acceleration factor of roughly 20 was used. The specific reconstruction strategies for DW-PRI with HYPR still need to be optimized further to minimize the errors in the reconstructed tensors and anisotropy maps. Despite this limitation, the method is still promising for high angular DW sampling using DW-PRI methods.

References:

[1] Jung KJ et al. MRM 19:349 (1991); [2] Gmitro AF et al. MRM 29:835 (1993); [3] Trouard TP et al. MRM 42:11 (1999); [4] Donald BM et al. ISMRM 2108 (2004); [5] Tuch DS et al. Neuron 40:885 (2003). [6] Mistretta CA et al. MRM (in press); [7] Hasan K et al. JMRI 13:769 (2001).

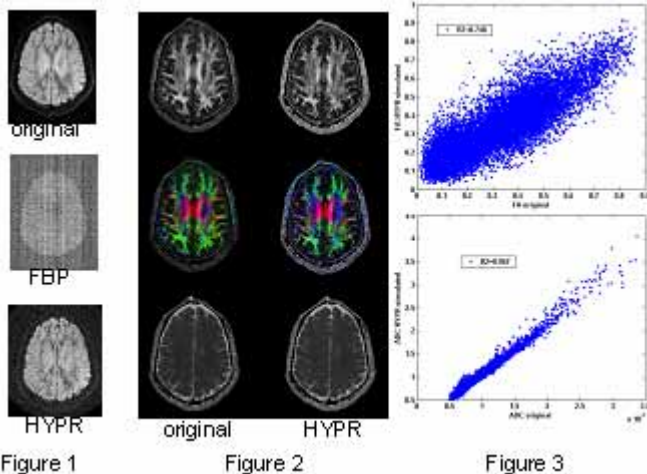


Figure 1. Comparison of original, FBP and HYPR reconstructed DW images for one encoding direction. The HYPR reconstruction clearly has less image artifacts.

Figure 2. Comparison of original and HYPR DTI maps: (top) FA; (middle) eigenvector color; (bottom) mean diffusivity)

Figure 3. Plots comparing the estimated FA and mean diffusivity between the original DTI data and HYPR over the region of the brain in Figure 2. The dispersion is relatively small for the mean diffusivity; but is significantly broader for the FA maps.